Colloids and Surfaces B: Biointerfaces 127 (2015) 130–136

Contents lists available at ScienceDirect

Colloids and Surfaces B: Biointerfaces

journal homepage: www.elsevier.com/locate/colsurfb

Quantum dots encapsulated glycopolymer vesicles: Synthesis, lectin recognition and photoluminescent properties

Danfeng Pei[a,b], Yanchun Li[c], Qingrong Huang[d], Qu Ren[e], Fan Li[a,*], Tongfei Shi[a,*]

[a] State Key Laboratory of Polymer Physics and Chemistry, Changchun Institute of Applied Chemistry, Chinese Academy of Sciences, Changchun 130022, PR China
[b] University of Chinese Academy of Sciences, Beijing 100049, PR China
[c] Department of Pediatric Respiratory Medicine, First Hospital of Jilin University, Changchun 130021, Jilin Province, PR China
[d] Food Science Department, Cook College, Rutgers University, New Brunswick, NJ 08901, United States
[e] Clinical Laboratory Center, Air Force General Hospital, No. 30 Fucheng Road, Haidian District, Beijing 100142, PR China

ARTICLE INFO

Article history:
Received 18 September 2014
Received in revised form 12 January 2015
Accepted 20 January 2015
Available online 28 January 2015

Keywords:
Glycopolymer vesicles
RAFT polymerization
Quantum dots
Lectin recognition
Targeted delivery
Fluorescent imaging

ABSTRACT

Biomimetic star-shaped glycopolymer poly(ε-caprolactone)-*b*-poly(2-aminoethyl methacrylate-*b*-poly(gluconamidoethylmethacrylate) (SPCL–PAMA–PGAMA) was synthesized by the combination of ring opening polymerization (ROP) and reversible addition-fragmentation chain transfer (RAFT) polymerization. The glycopolymer self-assembled into vesicles with low critical aggregation concentration (CAC) (0.0075 mg/mL). Then, the carboxylic capped CdTe QDs were encapsulated within the glycopolymer vesicles. The QDs encapsulated glycopolymer vesicles (Gly@QDs vesicles) could specifically bind Concanavalin A (Con A) without changing the photoluminescent properties of the Gly@QDs vesicles. Cell viability studies revealed that the cytotoxicity of the Gly@QDs vesicles was remarkably improved as compared to that of the original QDs. The Gly@QDs vesicles were internalized by Hep G2 cells and then emitted green fluorescence in the cells. Consequently, these Gly@QDs vesicles provided a multifunctional platform for targeted delivery and imaging.

1. Introduction

In recent years, amphiphilic block copolymers self-assembled vesicles (also referred to as polymersomes) have attracted rapidly growing interest due to their potential applicability in life science and biomedicine [1–4]. The vesicles can encapsulate various agents within the vesicles core or in the hydrophobic bilayer due to the hollow and spherical morphology [5–8]. However, in spite of the successful application of polymeric vesicles for delivery both *in vitro* and *in vivo*, one of the intractable problems is the lack of active targeting to specific tissues or organs, which leads to the decreased therapeutic efficacy. Moreover, it is important to identify the location of the vesicles after their uptake by cells, which can be achieved by using the imaging techniques, thereby providing precise evaluation of therapeutic efficacy. In this case, multifunctional vesicles for targeted delivery and imaging become important.

Targeted delivery can be achieved by using a variety of targeting ligands to functionalize the polymeric vesicles. The targeting ligands include small organic molecules, carbohydrates, aptamers, peptides and antibodies [9–11]. Among these targeting ligands, carbohydrates show highly specific interactions with endogenous lectin, a carbohydrate binding glycoprotein which is expressed on mammalian cell surfaces [12]. Synthetic glycopolymers containing carbohydrate moieties exhibit similar functionality to natural oligosaccharides [13–15]. However, only few reports are available on glycopolymer vesicles [16–18].

The fluorescence-based imaging technique has aroused significant interest in the area of biological applications [19,20]. QDs have received enormous applications in biomedical fields [21,22], owing to their high luminescence, single excitation narrow emission and low photo bleaching properties [23]. However, the cytotoxicity of QDs is still the major obstacle for their applications nowadays. Carbohydrates have been reported to improve the biocompatibility and bioactivity of QDs by covalent conjugation [24]. Thus, the glycopolymer vesicles are expected to reduce the toxicity of the QDs. Moreover, the embedded QDs may turn the glycopolymer vesicles into a potential fluorescent probe for identifying the location of the glycopolymer vesicles after their uptake by cells.

Herein, biomimetic glycopolymer vesicles embedded with QDs were designed. On the one hand, the embedded QDs turned the

* Corresponding authors. Tel.: +86 431 85262137.
E-mail addresses: fli1216@ciac.ac.cn (F. Li), tfshi@ciac.ac.cn (T. Shi).

http://dx.doi.org/10.1016/j.colsurfb.2015.01.032
0927-7765/

glycopolymer vesicles into a potential fluorescent probe; on the other hand, the glycopolymer vesicles were expected to improve the biocompatibility of the QDs. To archive this goal, the biomimetic star-shaped SPCL–PAMA–PGAMA glycopolymer was synthesized by the combination of ROP and RAFT polymerization. The glycopolymer self-assembled into vesicles in phosphate buffered saline (PBS) and were characterized by transmission electron microscopy (TEM) and dynamic light scattering (DLS). Then, the glycopolymer vesicles were decorated with QDs. The photoluminescent properties of the Gly@QDs vesicles were characterized by the luminescence spectrometer. The recognition properties of the Gly@QDs vesicles with Con A were investigated at room temperature by measuring the turbidity. Cell internalization and cytotoxicity of the Gly@QDs vesicles were studied by fluorescence microscopy and MTT assay, respectively.

2. Experimental

2.1. Materials

Stannous octoate ($SnOct_2$), 4-(dimethylamino) pyridine (DMAP), *N*,*N*-dicyclohexylcarboiimide (DCC), 4-cyano-4-(phenylcarbonothioylthio) pentanoic acid (CTP), D-gluconolactone, ethanolamine hydrochloride, dimethylsulfoxide (DMSO), mercaptoacetic acid (TGA), 1-ethyl-3-(3-dimethylaminopropyl) carbodiimide hydrochloride (EDC), *N*-hydroxysuccinimide (NHS), Dubelcco's modified Eagle's medium (DMEM), fetal bovine serum (FBS) were all purchased from Sigma-Aldrich and used as received. Methacryloyl chloride, cadmium chloride, sodium borohydride and tellurium powder were all purchased from Aladdin and used as received. ε-Caprolactone (Sigma-Aldrich), toluene (Beijing Chemical Reagent Co., Ltd.) and dichloromethane (DCM) (Beijing Chemical Reagent Co., Ltd.) were dried over CaH_2 and distilled prior to use. Pentaerythritol from Sinopharm chemical reagent company was recrystallized from water. 2-Aminoethyl methacrylate hydrochloride (AMA·HCl) was synthesized from ethanolamine hydrochloride and methacryloyl chloride according to the literature procedure (72.0% yield) [25]. D-Gluconamidoethyl methacrylate glycomonomer (GAMA) was synthesized from D-gluconolactone and 2-aminoethyl methacrylate hydrochloride according to the literature procedure (70.0% yield) [25]. TGA capped CdTe QDs (1 μM in water, emission maxima wavelength and full-width at half-maximum (FWHM) are 554 nm and 75 nm at 360 nm of excitation, respectively) were prepared according to the literature procedure [26].

2.2. Synthesis of biomimetic star-shaped SPCL–PAMA–PGAMA glycopolymer by the combination of ROP and RAFT polymerization

The biomimetic star-shaped SPCL–PAMA–PGAMA glycopolymer was prepared as shown in Scheme 1. According to the literature [27], four arms star-shaped PCL with four hydroxyl end groups (SPCL-OH) was synthesized by ROP of ε-caprolactone monomer using pentaerythritol as an initiator and stannous octoate as a catalyst at 110 °C for 24 h. After cooling to room temperature, the crude product was dissolved in DCM and precipitated into methanol to give white solid. The solid was dried in vacuum to constant weight in a yield of 95.0%. ^{1}H NMR (400 MHz, $CDCl_3$, δ) of $SPCL_{27}$-OH sample: 1.38 (m, 54*H*, —$COCH_2CH_2C\mathbf{H_2}CH_2CH_2O$—), 1.63 (m, 108*H*, —$COCH_2C\mathbf{H_2}CH_2C\mathbf{H_2}CH_2O$—), 2.28 (m, 54*H*, —$COC\mathbf{H_2}CH_2$ $CH_2CH_2CH_2O$—), 3.65 (t, 2*H*, —$C\mathbf{H_2}OH$), 4.05 (m, 54*H*, —$COCH_2CH_2CH_2CH_2C\mathbf{H_2}O$—).

Subsequently, the SPCL-OH was converted into macro-RAFT agent (SPCL-CTP) *via* esterification with CTP. $SPCL_{27}$-OH precursor (1.10 g, 0.1 mmol), CTP (279.38 mg, 1 mmol) and DMAP (12.22 mg, 0.1 mmol) were dissolved in DCM (5 mL) and cooled to 0 °C Then, DCC (247.60 mg, 1.2 mmol) was dissolved in DCM (1 mL) and added dropwise into the reaction mixture. The mixture was stirred in the dark at room temperature for 60 h. Dicyclohexylurea was removed by filtration, the filtrate was concentrated and precipitated into methanol under vigorous stirring. The pink solid was filtered and dried under reduced pressure (92.0% yield). ^{1}H NMR (400 MHz, $CDCl_3$, δ) of $SPCL_{27}$-CTP sample: 1.38 (m, 54*H*, —$COCH_2CH_2C\mathbf{H_2}CH_2CH_2O$—), 1.63 (m, 108*H*, —$COCH_2C\mathbf{H_2}CH_2C\mathbf{H_2}CH_2O$—), 1.86 (s, 3*H*, —$C(CN)(C\mathbf{H_3})$—), 2.28 (m, 54*H*, —$COC\mathbf{H_2}CH_2CH_2CH_2CH_2O$—), 2.31–2.64 (t, 4*H*, —$C\mathbf{H_2}C\mathbf{H_2}COO$—), 4.05 (m, 54*H*, —$COCH_2CH_2CH_2CH_2C\mathbf{H_2}O$—), 7.3–7.8 (t, 5*H*, Ar**H**).

Finally, the SPCL–PAMA–PGAMA glycopolymer was synthesized by the RAFT polymerization of AMA·HCl and GAMA using SPCL-CTP as the macro-RAFT agent in one pot. $SPCL_{27}$-CTP (216.00 mg, 0.02 mmol), AMA·HCl (135.00 mg, 0.8 mmol) and AIBN (2.624 mg, 0.016 mmol) were dissolved in DMSO (1 mL). The solution was degassed by three freeze-evacuate-thaw cycles and polymerized at 60 °C for 5 h. Then a degassed solution of GAMA (370.00 mg, 1.2 mmol) in DMSO (1 mL) was transferred into the stirred reaction mixture directly, without adding further AIBN initiator. The polymerization was typically terminated after 3 h by exposure to air. The pink crude product was precipitated into 2-propanol, washed three times with warm methanol, and then dried under reduced pressure. The yield was 69.4%. ^{1}H NMR (400 MHz, DMSO-d_6, δ) of $SPCL_{27}$–$PAMA_{10}$–$PGAMA_{11}$ sample: 0.6–1.0 (m, 63*H*, —$C(C\mathbf{H_3})$ —), 1.6–2.0 (m, 42*H*, —$C(C\mathbf{H_2})$—), 1.38 (m, 54*H*, —$COCH_2CH_2C\mathbf{H_2}CH_2CH_2O$—), 1. 63 (m, 108*H*, —$COCH_2C\mathbf{H_2}CH_2C\mathbf{H_2}CH_2O$—), 1.86 (s, 3*H*, —$C(CN)(C\mathbf{H_3})$—), 2.28 (m, 54*H*, —$COC\mathbf{H_2}CH_2CH_2CH_2CH_2O$—), 2.31–2.64 (t, 4*H*, —$C\mathbf{H_2}C\mathbf{H_2}COO$—), 4.05 (m, 54*H*, —$COCH_2CH_2CH_2CH_2C\mathbf{H_2}O$—), 3.00–3.75 and 4.02–4.63 (glucose residue).

2.3. Formation of SPCL–PAMA–PGAMA glycopolymer vesicles

Typically, $SPCL_{27}$–$PAMA_{10}$–$PGAMA_{11}$ (10 mg) was dissolved in DMSO (1 mL). Then PBS (pH = 7.4) was added dropwise at a rate of 1 mL/min under stirring until the appearance of a blue tint. Then, the solution was dialyzed against PBS for 48 h (MWCO = 12000). The morphology and the size of the formed glycopolymer vesicles were characterized by TEM and DLS.

The critical aggregation concentration (CAC) was determined by using pyrene as a fluorescence probe. Steady state fluorescence spectra were obtained by a Shimadzu RF5301 luminescence spectrometer.

2.4. Preparation of Gly@QDs vesicles and their lectin recognition properties

QDs solution (2 mL) was added to PBS solution (pH = 7.4, 1 mL) of EDC (2.6 mg) and NHS (1.5 mg). The reaction mixture was stirred for 30 min at room temperature. Then the $SPCL_{27}$–$PAMA_{10}$–$PGAMA_{11}$ glycopolymer solution (10.0 mg in 10 mL of PBS) was added to the above PBS solution [24]. After stirring the reaction mixture overnight at room temperature, the mixture was purified by centrifuge for 30 min at 6000 rpm twice and redispersed in PBS at a concentration of 1 mg/mL.

The recognition properties of the Gly@QDs vesicles with Con A were investigated at room temperature and measured by UV–vis spectrophotometer at 360 nm to determine the turbidity [27].

2.5. Cellular uptake

Fluorescence microscopy was performed to determine the uptake of Gly@QDs vesicles by Hep G2 cells. The cells were seeded

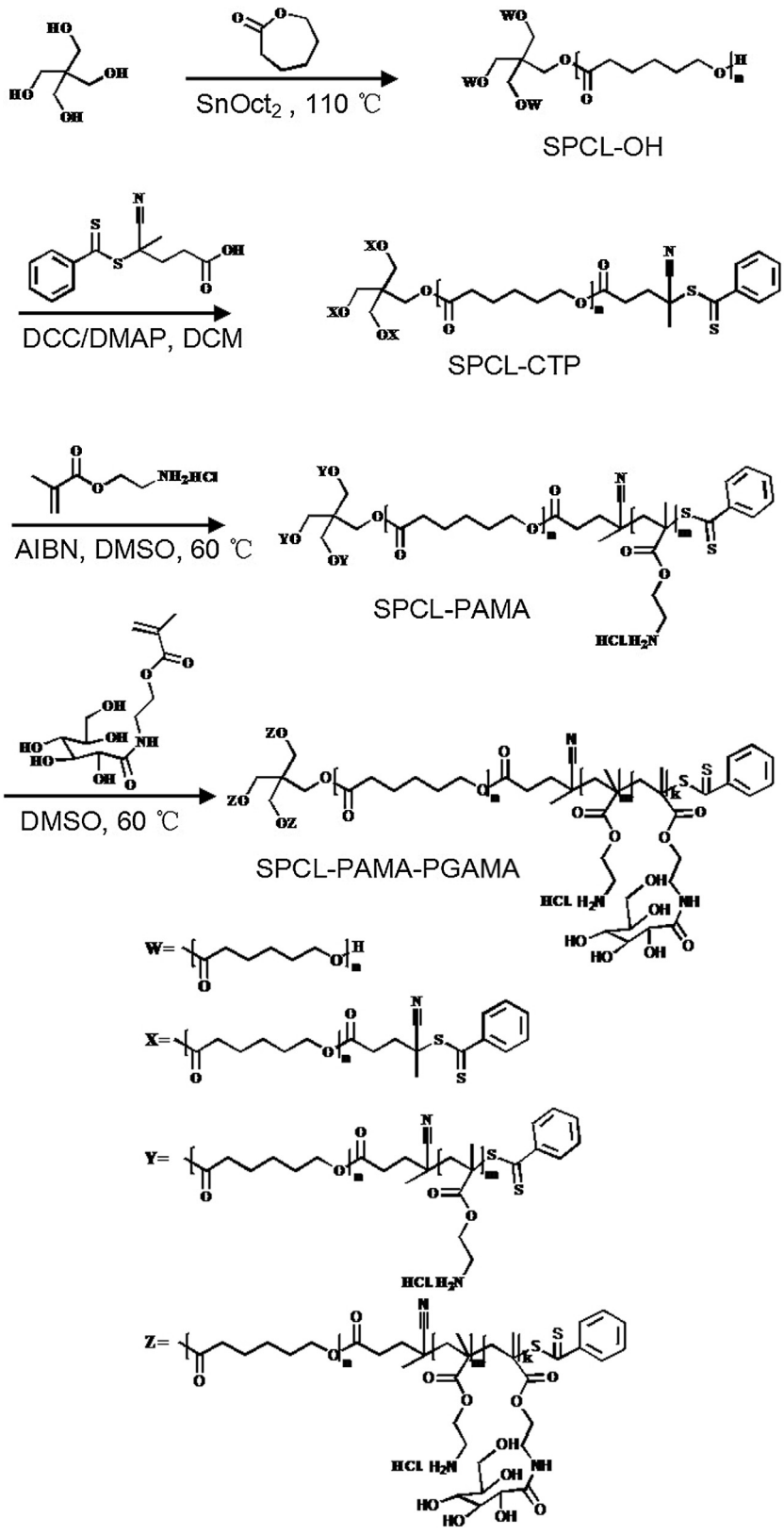

Scheme 1. Synthesis of biomimetic star-shaped SPCL–PAMA–PGAMA glycopolymer by the combination of ROP and RAFT polymerization.

in a 6-well plate at a density of 2×10^4 cells per well. After 24 h incubation, the cells were treated with Gly@QDs vesicles containing 80 nM QDs for 4 h. After incubation, the growth medium was removed, and the cells were washed several times with PBS. Then, the cells were observed under fluorescence microscopy.

2.6. Cytotoxicity measurements

The cytotoxicity of QDs and Gly@QDs vesicles against Hep G2 cells was evaluated *in vitro* by MTT assay. Hep G2 cells were seeded in a 96-well plate with a density of 6000 cells per well and incubated in DMEM (100 μL) for 24 h. The medium was then replaced with 100 μL of serial dilutions of QDs or Gly@QDs vesicles solutions in DMEM. The cells grew for another 24 h. Then, 10 μL of MTT solution in PBS with the concentration of 5 mg/mL was added and the plate was incubated for another 4 h at 37 °C. After that, the medium containing MTT was removed and 150 mL of DMSO was added to each well to dissolve the MTT formazan crystals. Finally, the plate was shaken for 10 min, and the absorbance of formazan product was measured at 492 nm with a Perlong-DNM-9602 microplate reader.

3. Results and discussion

3.1. Synthesis and characterization of biomimetic star-shaped SPCL–PAMA–PGAMA glycopolymer

RAFT polymerization offers a robust strategy for the synthesis of well-defined glycopolymers [28,29]. Biomimetic star-shaped $SPCL_{27}$–$PAMA_{10}$–$PGAMA_{11}$ glycopolymer was synthesized by the combination of ROP of ε-caprolactone and RAFT polymerization of AMA·HCl and GAMA, as illustrated in Scheme 1. The molecular weight, molecular weight distribution and molecular structure could be determined by ^{1}H NMR (Fig. 1), GPC (Fig. S1) and FT-IR (Fig. S2), respectively. Fig. 1(C) showed the ^{1}H NMR spectra of the $SPCL_{27}$–$PAMA_{10}$–$PGAMA_{11}$ glycopolymer. Characteristic proton signals concerning to PCL, PAMA and PGAMA segments were assigned (Fig. 1(C)). The number average molecular weight (M_n) of the $SPCL_{27}$–$PAMA_{10}$–$PGAMA_{11}$ glycopolymer calculated from ^{1}H NMR was 31.400 g/mol. The symmetrical and unimodal GPC curve (Fig. S1) showed that the $SPCL_{27}$–$PAMA_{10}$–$PGAMA_{11}$ glycopolymer possessed a narrow molecular weight distribution (PDI = 1.13). The FT-IR spectra of the $SPCL_{27}$–$PAMA_{10}$–$PGAMA_{11}$ glycopolymer (Fig. S2) showed a broad band at 3412 cm^{-1}, which was assigned to the stretching vibration of -OH group of the PGAMA block. The characteristic bending vibration of -NH_2 and -NH group at 1648 cm^{-1} and 1547 cm^{-1} assignable to the PAMA and PGAMA block was observed, respectively.

3.2. Preparation and characterization of biomimetic glycopolymer vesicles

The obtained biomimetic $SPCL_{27}$–$PAMA_{10}$–$PGAMA_{11}$ glycopolymer self-assembled into vesicles in PBS. The symmetrical and unimodal DLS curve indicated a narrow size distribution of the glycopolymer vesicles with the average diameter of 59 nm (Fig. 2(A)). TEM showed that the glycopolymer vesicles possessed a hollow and spherical structure in PBS (Fig. 3(A)) with a diameter of 42 ± 3 nm.

The CAC value is an important parameter to evaluate the stability of the glycopolymer vesicles. A low CAC value means a stable structure in diluted solution. The CAC value of the vesicles was investigated by fluorescence spectra using pyrene as a hydrophobic probe. The ratios of the intensities at 384 nm and 373 nm (I_{384}/I_{373}) of the excitation spectra were analyzed as a function of glycopolymer concentration. The CAC value was taken from the intersection

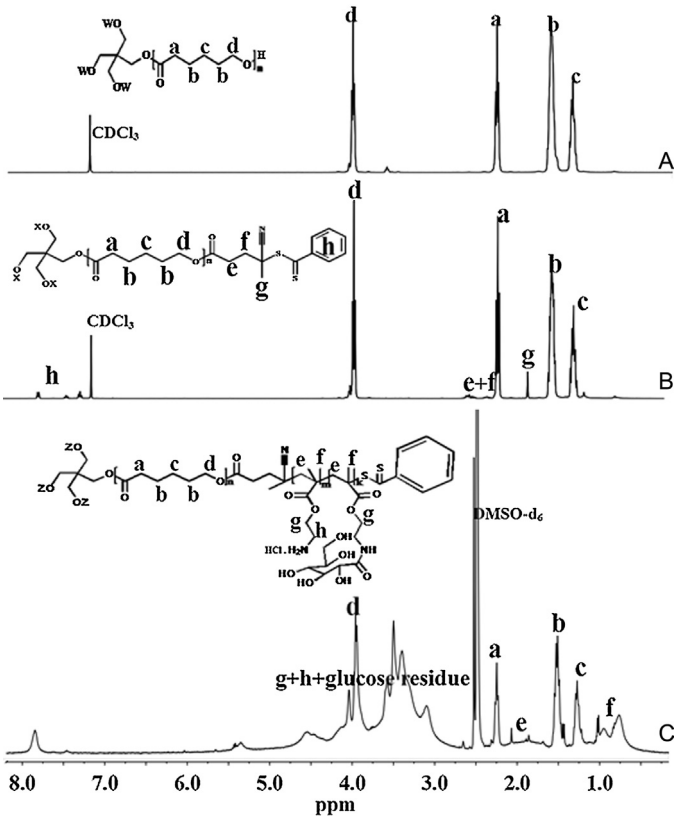

Fig. 1. ^{1}H NMR spectra of SPCL-OH (A) in $CDCl_3$, SPCL-CTP (B) in $CDCl_3$ and SPCL–PAMA–PGAMA (C) in DMSO-d_6.

of the tangent to the curve at the inflection with the horizontal tangent though the points at the low concentrations [30]. The CAC value of the $SPCL_{27}$–$PAMA_{10}$–$PGAMA_{11}$ glycopolymer was 0.0075 mg/mL. The low CAC value indicated that the glycopolymer vesicles possessed good stability in PBS and could prevent dissociation upon sudden dilution.

3.3. Preparation and characterization of Gly@QDs vesicles and their recognition properties

Water soluble CdTe QDs containing carboxylic groups were used in this study. Some of the carboxylic groups on the surface of QDs were activated by using the NHS/EDC coupling method in PBS and subsequently reacted with the primary amino groups on the glycopolymer. The QDs loading content could be controlled by changing the mole ratio of the glycopolymer to QDs. The size of the Gly@QDs vesicles calculated from DLS was about 72 nm (Fig. 2(A)). The size was a little larger than that of the original glycopolymer vesicles (Fig. 2(A)), which confirmed the successful conjugation of the QDs to the glycopolymer vesicles. The DLS curve of the Gly@QDs vesicles was unimodal, indicating no aggregates formed after the conjugation. Fig. 3(B–D) showed the morphology of the Gly@QDs vesicles. At low magnification (Fig. 3(B)), the QDs were too tiny to be observed, but it could be used to calculate the size of the Gly@QDs vesicles. The size counted from Fig. 3(B) was 46 ± 2.7 nm. In Fig. 3(C and D), we could clearly see that the QDs were distributed on the vesicles wall.

Fluorescence spectra of the Gly@QDs vesicles and QDs were recorded on a luminescence spectrometer (Fig. 4(A)). The emission intensity of the Gly@QDs vesicles was weakened as compared to that of the original QDs. The fluorescence quenching may be caused by the amidation reaction for the preparation of Gly@QDs vesicles or the encapsulation of QDs within the glycopolymer vesicles.

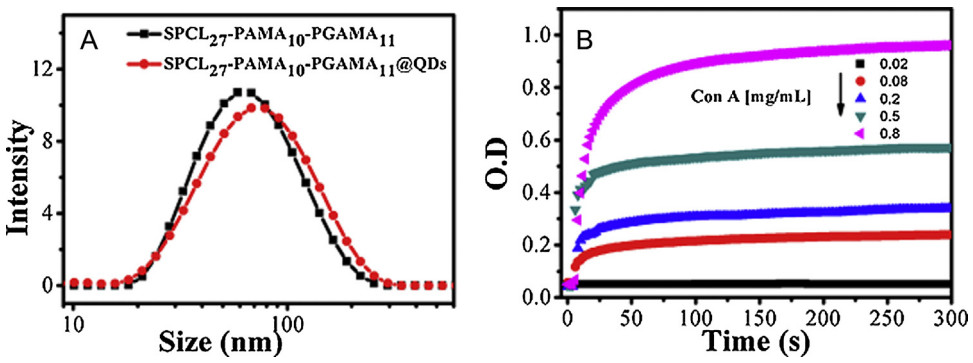

Fig. 2. (A) The particle size and the size distribution of the vesicles: $SPCL_{27}$–$PAMA_{10}$–$PGAMA_{11}$ (1 mg/mL) and $SPCL_{27}$–$PAMA_{10}$–$PGAMA_{11}$@QDs (1 mg/mL). (B) The interactions of Con A with Gly@QDs vesicles (0.05 mg/mL) at pH = 9.18.

Moreover, the emission maxima wavelength was slightly red shift. This was due to the fluorescence resonance energy transfer (FRET) between the CdTe QDs in the Gly@QDs vesicles. The FRET was sensitive to molecular rearrangements on the 1–10 nm range [31]. The red shift of the emission maxima wavelength indicated that several QDs were encapsulated within a vesicle successfully.

The specific recognition properties of the Gly@QDs vesicles with lectin were studied. It is reported that Con A specifically recognizes D-glucopyranoside and D-mannopyranoside residues with free 3-, 4-, and 6-hydroxyl groups, and the binding of Con A with gluconolactone-based glycopolymer usually results in the Con A-cross-linked aggregates [32,33]. The interactions between the Gly@QDs vesicles and Con A were investigated at room temperature and measured by UV–vis spectrophotometer to determine the turbidity. In order to determine the specific recognition properties, bovine serum albumin (BSA) was selected as a control. In Fig. S3(A) the Gly@QDs vesicles could bind both Con A and BSA to form the aggregates in PBS (pH = 7.4). We speculated that

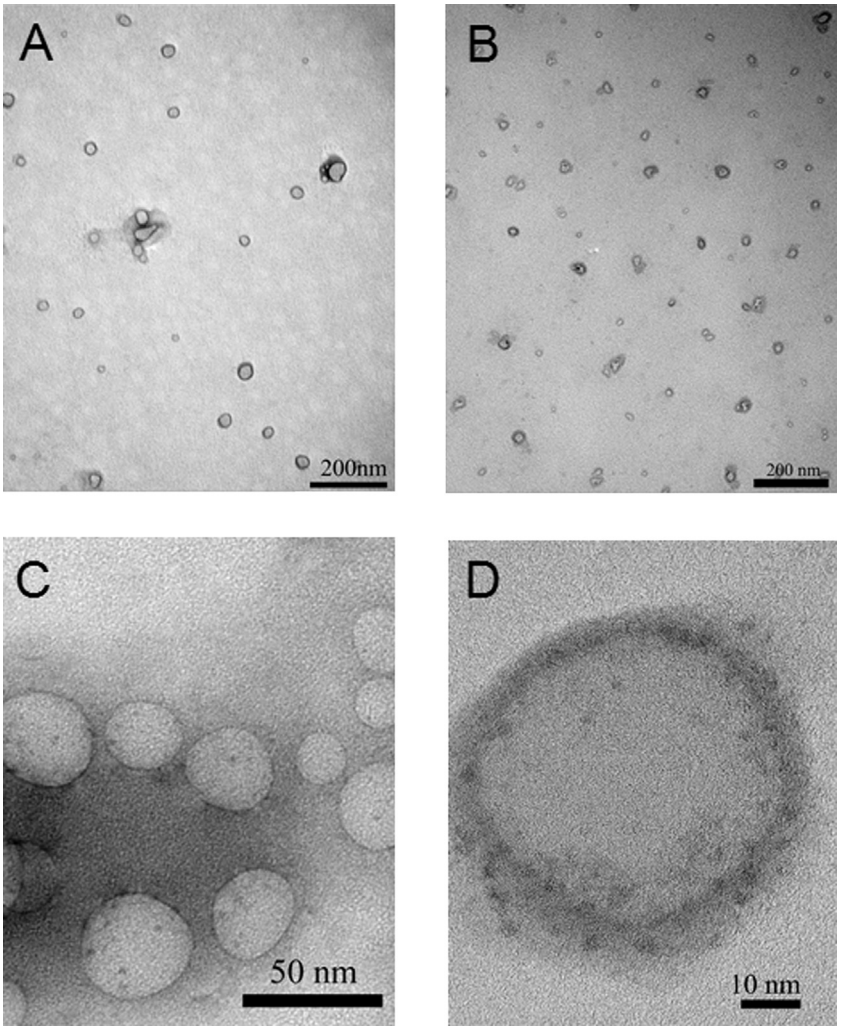

Fig. 3. TEM photographs of the vesicles: $SPCL_{27}$–$PAMA_{10}$–$PGAMA_{11}$ (A) and Gly@QDs (B, C and D).

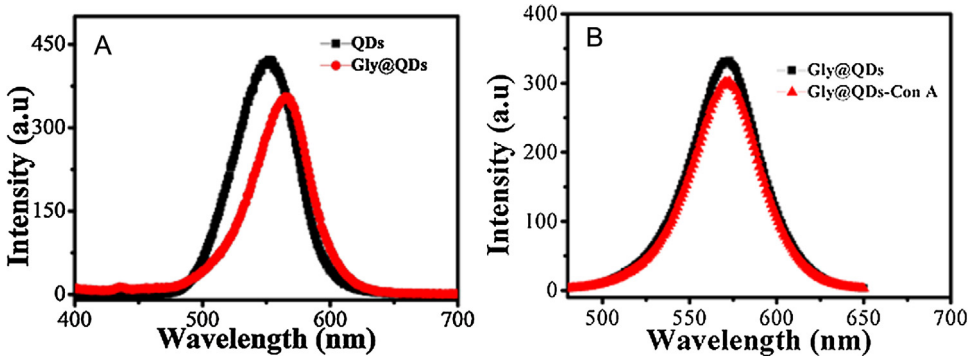

Fig. 4. (A) The photoluminescence spectra of the original QDs and Gly@QDs vesicles (at 360 nm of excitation). (B) The photoluminescence spectra of the Gly@QDs vesicles and Gly@QDs-Con A aggregates (at 360 nm of excitation).

the results may be caused by the electrostatic interactions. The Gly@QDs vesicles were positively charged (ζ potential = 13 mV), while the proteins (ζ potential = −6 mV for Con A and ζ potential = −9 mV for BSA) were negatively charged in PBS. To verify our conjecture, we adjusted the solution pH to 9.18. At this pH, both the Gly@QDs vesicles (ζ potential = −3 mV) and the proteins were negatively charged (ζ potential = −19 mV for Con A and ζ potential = −15 mV for BSA), thus there were no electrostatic interactions. Excitingly, the Gly@QDs vesicles specifically bound Con A (Fig. S3(A)). There were no interactions between the Gly@QDs vesicles and BSA (Fig. S3(A)). Then, we investigated the recognition process at pH = 9.18, particularly. A series of experiments with different concentration of Con A/BSA were performed. UV–vis spectroscopy and DLS were used to investigate the process. The UV–vis spectra (Fig. 2(B)) showed that the turbidity of the Gly@QDs-Con A solution was concentration dependent. At the consistent Gly@QDs vesicles concentration, when the concentration of Con A below 0.02 mg/mL, no changes on the turbidity were observed. When the concentration above 0.02 mg/mL, the turbidity increased immediately after Con A added. Meanwhile, as the concentration of Con A increased, the extent of turbidity also increased. The increased turbidity may be caused by the formation of larger Con A-cross-linked aggregates. DLS results confirmed the suspicion. As shown in Fig. S3(B), as the concentration of Con A increased from 0 mg/mL to 0.8 mg/mL, the size of the aggregates increased from about 72 nm to 800 nm. Moreover, we monitored the stability of the formed Con A-cross-linked aggregates. As shown in Fig. S3(C), no obvious changes on the turbidity was observed in 3 h. The size of the aggregates was remain the same after 24 h. As contrast, when we added different concentration of BSA to the Gly@QDs vesicle solution, the turbidity and the particles size (Fig. S4) did not change. The results suggested that the binding between Gly@QDs vesicles and Con A occurred and resulted in stable Con A-cross-linked aggregates, which provided them useful for targeted delivery.

As shown in Fig. S3(A), the Gly@QDs vesicles could specifically recognize Con A. It was important to evaluate if the luminescent properties were influenced when the Gly@QDs vesicles were used as targeted delivery vehicles. Thus, we measured the fluorescence spectra of the Gly@QDs-Con A aggregates. Fortunately, the luminescence intensity and the emission maxima wavelength were not significantly changed when the Gly@QDs-Con A aggregates formed (Fig. 4(B)).

3.4. Cell internalization and the in vitro cytotoxicity measurements

Fluorescence microscopy was performed to determine the uptake of the Gly@QDs vesicles by Hep G2 cells and the cell uptake with the original QDs was performed as a negative control. The images showed the uptake after 4 h of incubation. Green fluorescence was emitted in the cells. The fluorescent image obtained was overlapped on a bright field image to determine the site of the original QDs (Fig. S5) and Gly@QDs vesicles in the cells (Fig. 5(A)). Both the original QDs and the Gly@QDs vesicles were found to be mostly localized in the cytoplasm of the cells. Dot-shaped fluorescence was observed within the cytoplasm, which suggested that both the original QDs and the Gly@QDs vesicles were internalized through an endocytosis pathway [34].

The cytotoxicity of the Gly@QDs vesicles was evaluated against Hep G2 cells by MTT assay. The viability of Hep G2 cells after incubation with Gly@QDs vesicles (containing a consistent glycopolymer concentration (100 μg/mL, at this concentration the cytotoxicity was low as shown in Fig. S6)) and original QDs at different QDs dosage from 10 nM to 160 nM was showed in Fig. 5(B). For the original QDs, the cell viability was only 33.4% when the concentration of QDs was 160 nM, indicating a significant toxicity of the original QDs. However, the cell viability of the Gly@QDs vesicles was above 70% at this concentration. The Gly@QDs vesicles showed a remarkably

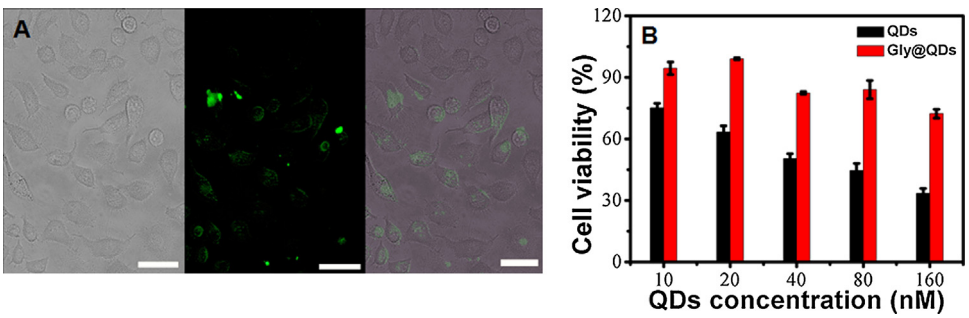

Fig. 5. (A) Representative white and fluorescent images of Hep G2 cells incubated with Gly@QDs vesicles. (The scale bar is 50 μm) and (B) Viability of Hep G2 cells after incubation with QDs and Gly@QDs vesicles at various QDs dosage with consistent glycopolymer concentration (100 μg/mL.)

improved cytotoxicity than that of the original QDs. The glycopolymer vesicles seemed to mask the surface of QDs and prevented the release of QDs efficiently, thus accounting for the lower toxicity. The Gly@QDs vesicles may be suitable to use as potential *in vivo* fluorescent probe for identifying tumor location.

4. Conclusions

We have successfully designed the novel QDs encapsulated gluconolactone-based glycopolymer vesicles and investigated their lectin recognition and photoluminescent properties. To achieve this goal, the biomimetic star-shaped $SPCL_{27}$–$PAMA_{10}$–$PGAMA_{11}$ glycopolymer was synthesized by the combination of ROP and RAFT polymerization for the first time. The glycopolymer self-assembled into vesicles with narrow size distribution and low CAC. Then, CdTe QDs were used to conjugate with the PAMA block to turn the glycopolymer vesicles into a potential fluorescent probe. The emission maxima wavelength of the Gly@QDs vesicles was red shift due to the occurrence of FRET between the CdTe QDs in the Gly@QDs vesicles. The Gly@QDs vesicles could specifically bind Con A without changing the luminescent properties of the Gly@QDs vesicles. Cell viability studies revealed that the glycopolymer vesicles remarkably improved the biocompatibility of QDs. The Gly@QDs vesicles were internalized by Hep G2 cells through an endocytosis pathway and then green fluorescence was emitted in the cells. Consequently, these Gly@QDs vesicles provided a multifunctional platform for targeted delivery and imaging.

Acknowledgments

This work is supported by the National Natural Science Foundation of China (grant nos. 51028301494, 21174146 and 81100014). Programs and subsidized by the Special Funds for National Basic Research Program of China (grant no. 2009CB930100).

Appendix A. Supplementary data

Supplementary data associated with this article can be found, in the online version, at http://dx.doi.org/10.1016/j.colsurfb.2015.01.032.

References

[1] D.A. Christian, S. Cai, D.M. Bowen, Y. Kim, J.D. Pajerowski, D.E. Discher, Eur. J. Pharm. Biopharm. 71 (2009) 463–474.
[2] R.P. Brinkhuis, F.P.J.T. Rutjes, J.C.M. van Hest, Polym. Chem. 2 (2011) 1449–1462.
[3] P. Tanner, P. Baumann, R. Enea, O. Onaca, C. Palivan, W. Meier, Acc. Chem. Res. 44 (2011) 1039–1049.
[4] P.V. Pawar, S.V. Gohil, J.P. Jain, N. Kumar, Polym. Chem. 4 (2013) 3160–3176.
[5] O. Onaca, R. Enea, D.W. Hughes, W. Meier, Macromol. Biosci. 9 (2009) 129–139.
[6] T. Caon, L.C. Porto, A. Granada, M.P. Tagliari, M.A.S. Silva, C.M.O. Simoes, R. Borsali, V. Soldi, Eur. J. Pharm. Sci. 52 (2014) 165–172.
[7] J.S. Lee, J. Feijen, J. Control. Release 161 (2012) 473–483.
[8] B. Surnar, M. Jayakannan, Biomacromolecules 14 (2013) 4377–4387.
[9] T.O. Pangburn, M.A. Petersen, B. Waybrant, M.M. Adil, E. Kokkoli, J. Biomech. Eng. 131 (2009) 074005.
[10] M.S. Kim, D.W. Lee, K. Park, S.J. Park, E.J. Choi, E.S. Park, H.R. Kim, Colloids Surf., B: Biointerfaces (2014) 17–25.
[11] Y.C. Chen, C.F. Chiang, L.F. Chen, P.C. Liang, W.Y. Hsieh, W.L. Lin, Biomaterials 35 (2014) 4066–4081.
[12] J.F. Kennedy, P.M.G. Palva, M.T.S. Corella, M.S.M. Cavalcanti, L.C.B.B. Coelho, Carbohydr. Polym. 26 (1995) 219–230.
[13] S.R.S. Ting, G.J. Chen, M.H. Stenzel, Polym. Chem. 1 (2010) 1392–1412.
[14] C.R. Becer, Macromol. Rapid Commun. 33 (2012) 742–752.
[15] K.Y. Peng, M.Y. Hua, R.S. Lee, Carbohydr. Polym. 99 (2014) 710–719.
[16] A.M. Eissa, M.J.P. Smith, A. Kubilis, J.A. Mosely, N.R. Cameron, J. Polym. Sci., Part A: Polym. Chem. 51 (2013) 5184–5193.
[17] K. Aissou, A. Pfaff, C. Giacomell, C. Travelet, A.H.E. Muller, R. Borsal, Macromol. Rapid Commun. 32 (2011) 912–916.
[18] T. Kakuchi, R. Borsali, Langmuir 26 (2010) 2325–2332.
[19] R. Cicchi, F.S. Pavone, Anal. Bioanal. Chem. 400 (2011) 2687–2697.
[20] R.C. Han, Z.H. Li, Y.Y. Fan, Y.Q. Jiang, J. Genet. Genomics 40 (2013) 583–595.
[21] D. Bera, L. Qian, T.K. Tseng, P.H. Holloway, Materials 3 (2010) 2260–2345.
[22] H. Kim, C.Y.W. Ng, W.R. Algar, Langmuir 30 (2014) 5676–5685.
[23] C.B. Murray, D.J. Norris, M.G. Bawendi, J. Am. Chem. Soc. 115 (1993) 8706–8715.
[24] X.Z. Jiang, M. Ahmed, Z.C. Deng, R. Narain, Bioconjugate Chem. 20 (2009) 994–1001.
[25] R. Narain, S. Armes, Biomacromolecules 4 (2003) 1746–1758.
[26] H. Zhang, Z. Zhou, B. Yang, M.Y. Gao, J. Phys. Chem. B 107 (2003) 8–13.
[27] X.H. Dai, C.M. Dong, Polym. Sci., Part A: Polym. Chem. 46 (2008) 817–829.
[28] J. Bernard, X.J. Hao, T.P. Davis, C. Barner-Kowollik, M.H. Stenzel, Biomacromolecules 7 (2006) 232–238.
[29] A. Ghadban, L. Albertin, Polymers 5 (2013) 431–526.
[30] J. Aguiar, P. Carpena, J.A. Molina-Bolivar, C.C. Ruiz, J. Colloid Interface Sci. 258 (2003) 116–122.
[31] I.L. Medintz, H.T. Uyeda, E.R. Goldman, H. Mattoussi, Nat. Mater. 4 (2005) 435–446.
[32] C.H. Lu, X.S. Chen, Z.G. Xie, T.C. Lu, X. Wang, J. Ma, X.B. Jing, Biomacromolecules 7 (2006) 1806–1810.
[33] L.C. You, F.Z. Lu, Z.C. Li, W. Zhang, F.M. Li, Macromolecules 36 (2003) 1–4.
[34] Y. Bae, S. Fukushima, A. Harada, K. Kataoka, Angew. Chem. Int. Ed. 42 (2003) 4640–4643.